HHS Public Access

Author manuscript

*Nanomedicine*. Author manuscript; available in PMC 2016 April 01.

Published in final edited form as:

*Nanomedicine*. 2015 April ; 11(3): 559–567. doi:10.1016/j.nano.2014.11.011.

# Promoting filopodial elongation in neurons by membrane-bound magnetic nanoparticles

**Wolfgang Pita-Thomas, PhD**[1,2] **[Postdoctoral Fellow]**, **Michael B. Steketee, PhD**[1,3] **[Assistant Professor]**, **Stavros N. Moysidis**[1] **[Medical Student]**, **Kinjal Thakor**[1] **[Undergraduate student]**, **Blake Hampton**[1] **[Medical Student]**, and **Jeffrey L. Goldberg, MD, PhD**[1,4,*] **[Professor and Director of Research]**

[1]Bascom Palmer Eye Institute and Interdisciplinary Stem Cell Institute, University of Miami Miller School of Medicine, Miami, FL 33136

[2]Department of Anatomy and Neurobiology, Washington University, St. Louis, MO 63110

[3]Department of Ophthalmology and McGowan Institute for Regenerative Medicine, University of Pittsburgh, Pittsburgh, PA 15219

[4]Department of Ophthalmology, Shiley Eye Center, UC San Diego, San Diego, CA 92093

## Abstract

Filopodia are 5–10 μm long processes that elongate by actin polymerization, and promote axon growth and guidance by exerting mechanical tension and by molecular signaling. Although axons elongate in response to mechanical tension, the structural and functional effects of tension specifically applied to growth cone filopodia are unknown. Here we developed a strategy to apply tension specifically to retinal ganglion cell (RGC) growth cone filopodia through surface-functionalized, membrane-targeted superparamagnetic iron oxide nanoparticles (SPIONs). When magnetic fields were applied to surface-bound SPIONs, RGC filopodia elongated directionally, contained polymerized actin filaments, and generated retrograde forces, behaving as *bona fide* filopodia. Data presented here support the premise that mechanical tension induces filopodia growth but counter the hypothesis that filopodial tension directly promotes growth cone advance. Future applications of these approaches may be used to induce sustained forces on multiple filopodia or other subcellular microstructures to study filopodial on axon growth or cell migration.

### Keywords

Nanoparticles; filopodia; axon growth; mechanical tension

*Address correspondence to: Jeffrey L. Goldberg, M.D., Ph.D., Professor and Director of Research, Shiley Eye Center, UC San Diego, 9415 Campus Point Drive, La Jolla, CA 92093, P: (858) 534-9794, JLGoldberg@ucsd.edu.

**Competing financial interests:** The authors declare no competing financial interests

## Background

In the mammalian central nervous system (CNS), injured axons fail to regenerate, leading to permanent functional impairment as observed in glaucoma, stroke, or spinal cord or traumatic brain injury. This failure is multifactorial, attributable to a decline in intrinsic axon growth ability in adult neurons[1–3] and an unfavorable extracellular environment in the injured adult CNS.[4–7] Several approaches have begun to overcome these limitations in animal models resulting in some axon regeneration with partial functional recovery.[8–15] However, few axons regenerate, and these are prone to axon guidance errors.[16]

Axon growth rate and targeting are regulated by a specialized terminal region called the growth cone. Growth cones respond to environmental cues and exert mechanical forces against extracellular substrates to elongate the axon,[17–22] and application of mechanical tension to whole growth cones is sufficient to induce axon growth.[23–27] Growth cones are comprised of actin-rich filopodia and lamellipodia present at the growth cone periphery.[17, 28] Filopodia are 5–10 μm long structures produced by the polymerization of actin filaments against the inner plasma membrane.[17–19] Filopodia exert retraction forces that oppose elongation and shorten filopodia,[17, 20] but when filopodia bind to substrate through integrin membrane receptors, the resulting mechanical tension is hypothesized to transmit along the actin cytoskeleton to induce growth cone advance.[17, 20, 26, 29, 30] However, direct manipulation of filopodia to validate these hypotheses has proven difficult due to the small size of these structures. Here we have developed a strategy to apply mechanical tension specifically to the tip of growth cone filopodia of primary neurons through surface-functionalized, membrane-targeted superparamagnetic iron oxide nanoparticles (SPIONs). Using this technique, we test whether mechanical tension applied at the filopodia tip induces filopodia extension and whether linking filopodial retrograde forces to a substrate induces growth cone advance.

## Material and methods

### SPION functionalization and characterization

Coupling of 40 nm SPIONs were performed by Ocean Nanotech. Briefly, 0.2 mg of anti-Thy1 antibody (Millipore, Billerica, MA), or Cholera toxin b (Sigma-Aldrich, St Louis, MO) were coupled to 1 mg of 40 nm carboxyl iron oxide SPIONs (Ocean NanoTech, Springdale, AR) using the carbodiimide method. The SPION coupling was verified by agarose electrophoresis by the manufacturer. SPION hydrodynamic size and homogeneity after functionalization was measured using a Light Scattering Device (Wyatt Technology Corporation, Santa Barbara, CA).

### RGC culture, time-lapse recording and TEM microscopy

RGCs were cultured as previously described.[3, 31–33] Briefly, retinas were extracted from P0–P4 Sprague-Dawley rat pups and treated enzymatically with papain (Worthington, Freehold, NJ) before homogenization into a single cell suspension. RGCs were purified by immunopanning using negative selection by anti-macrophage antibody (AIA51240 Accurate chemical, Westbury, NY) and then a positive selection using an anti-Thy1antibody (clone

T11D7). RGCs were cultured on 35 mm glass bottom culture dishes (MatTek, Ashland, MA) or Formvar/Carbon Film Grids 100 meshes (Electron Miscroscope Sciences, Hatfield, PA) precoated with 10 μg/ml 70kDa poly-D-lysine (PDL) and 2 μg/ml laminin (Sigma) in Full-Sato medium prepared with Neurobasal or Hybernate (Life Technologies, Carlsbad, CA), 5 mg/mlinsulin, 1 mM sodium pyruvate, 1 mM L-glutamine, 5 mg/ml N-acetyl cysteine (NAC), 40 ng/ml triiodo-thyronine (Sigma), a homemade supplement similar to B27 prepared in Neurobasal using Sigma reagents,[33] 5 μM forskolin (Sigma), 50 ng/ml BDNF and 10 μg/ml CNTF (Peprotech, Rocky Hill, NY) at 37°C and 10% $CO_2$. Cultures were treated for 30 minutes with 40 μg/ml of the different 40 nm SPIONs or, 10 μl of anti-thy1 or anti-FITC 10 nm SPION (under the commercial name of Cd 90.1 and anti-FITC microbeads, Miltenyi Biotec, Bergisch-Gladbach, Germany). RGCs were recorded using a Zeiss DIC/fluorescence time-lapse microscope with a camera under the control of AxioVision software. Plan Apo 63x/1.40 DM objective with DIC optics was used for visualization. For video recording, a frame was taken every 30 msec.

For real-time labeling of F-actin filaments, RGCs were electroporated immediately after immunopanning as previously described[32] with the LifeAct vector (Ibidi, Martinsried, Germany)[34], seeded, and allowed to express the fluorescent peptide for one night. Fluorescent images were taken at 63x magnification with a Zeiss RFP filter.

For TEM, RGCs cultured on mesh grids were fixed with 2% glutaraldehyde (Electron Miscroscope Sciences) in PHEM buffer (600 mM PIPES, 25 mM HEPES, pH 6.9, 10 mM EGTA, 20 mM $MgCl_2$, and 7.4 mM NaCl) for two days at 4° C, stained with 2% osmium (Electron Miscroscope Sciences), dehydrated in incremental EtOH baths (20% for 30 seconds, 40% for 1 minute, 60% for 1 minute, 70% for 1.5 minutes, 80% for 1.5 minutes, 95% for 3 minutes, and 100% for 5 minutes), and then visualized with TEM (Philips CM10; FEI, Hillsboro, OR). To quantify the amount of SPIONs attached to RGC growth cones, the number of SPIONs per area outside the cell were counted using ImageJ and subtracted from the number of SPIONs per area at the growth cone. To obtain cell sections for TEM, RGCs were cultured over glass, fixed with Karnovsky fixative (30% glutaraldehyde, 12.5% paraformaldehyde, 50% cacodylate buffer from Electron Microscopy Science) for two days at 4° C, dehydrated through graded ethanol to absolute ethanol, as described above, and embedded in epon (Embed, Electron Microscopy Sciences) at 64°C. The glass coverslip was removed using hydrofluoric acid, and then semi-thin microtome sections were produced and then mounted on 150 mesh copper formvar-coated grids (Electron Microscopy Sciences). Sections were then visualized using the TEM methodology described above.

### Electromagnet settings and calibration

An electromagnet was constructed by machining a 1018 cold-rolled steel rod (Home Depot, Atlanta, GA) to the following dimensions: rear diameter: 8 mm by 17 cm length, middle diameter: 1.5 cm by 3 cm length, and front diameter: 0.5 cm by 2.5 cm length. The front diameter was then refined to a sharp end-point using a sand belt to allow a more focal magnetic field application and a higher magnetic gradient near the pole tip. This core was fit tightly into a 120/60 HT coil solenoid (216-758-1D, ASCO power technologies, Florham Park, NY) which was connected to a variable autotransformer voltage source (variable

autotransformer 0–100; Staco, Dayton, OH) and adapted to a micromanipulator (Narishige, Setagaya-Ku, Japan). The force was calibrated with 100 nm nanoparticles (Chemicell, Berlin, Germany) in glycerol (4080 centipoise or kg/(m*s); Sigma). To calibrate force, fluorescent time-lapse recordings of nanoparticles were recorded at electromagnet autotransformer settings of 15, 30, and 60. Stoke's law ($F=6\cdot\pi\cdot\eta\cdot R\cdot v$) was used to calculate the force at distances of ~5 to 100 μm from the electromagnet tip. A logarithmic relationship was observed between distance and force ($R^2 \geq 0.967$). Assuming that the iron oxide material isthe sa me within all SPIONs, the forces applied to 40nm and 10nm iron core SPIONsat different distances were calculated using the force values obtained for the fluorescent SPIONs and the formula ($F=V(M \cdot \nabla)B$) where V is the volume of the iron core, M is volumetric magnetization, and B is magnetic field. For some experiments, the tip of the magnet was dipped into a 50 μg/ml 70kDa PDL solution in water for 30 minutes and then into a 2 μg/ml laminin(Sigma) in Neurobasal for 4 hours.

## Results

For this study, we used two types of SPIONs with iron core diameters of either 10 or 40 nm. Due to the greater iron content, the larger SPIONs generated forces about 10-fold greater at 10–100 μm distances from our electromagnet tip (Fig. 1a). To target SPIONs to the RGC surface, we took advantage of GM1-ganglioside[35] and Thy-1[36] expression on RGC membranes by functionalizing SPIONs with moieties that bind these molecules specifically. Cholera Toxin B and anti-Thy1 antibody were chemically coupled to 40 nm SPIONs (Fig. 1b) and coupling efficiency was verified in a gel retention assay (Fig. 1c). After coupling, the SPION hydrodynamic diameter, measured by light scattering, increased in size and remained homogeneous; from 54±0.81 nm (non-functionalized SPION) to 55±1.71 nm with CtxB and 63.3±8 nm with anti-Thy1 antibody. We also analyzed commercial 10 nm iron oxide core SPIONs coupled to anti-Thy1 antibody or anti-FITC, the latter as a control was not expected to bind RGCs. We analyzed the effect of SPION functionalization on SPION attachment to RGC growth cone membranes using TEM, which revealed that significantly more SPIONs functionalized with anti-Thy1 or CtxB attached to RGC growth cones compared to non-functionalized or anti-FITC SPIONs (Fig. 2a–d). To discern the subcellular location of the SPIONs, we sectioned RGCs treated with 10 nm SPIONs. We observed that 30 minutes after addition to RGCs, SPIONs remained on the extracellular membrane without being endocytosed, and again the anti-Thy1 SPIONs demonstrated growth cone binding whereas the anti-FITC control SPIONs were not detected (Fig. 2e–h). Thus both 10 nm and 40 nm SPIONs can be directed to growth cone membranes using specific surface functionalizations.

Next we determined the cellular effect of applying magnetic forces to SPION-bound RGC growth cones. With either 40 nm anti-Thy1 or CtxB SPIONs, focal magnetic fields in the range of 5–50 pN/particle induced membrane and cytoplasmic accumulation at filopodial tips (Fig 3a, B, supplementary videos 1 and 2), consistent with SPION movement and accumulation. This indicates that SPION linkage to the membrane was of sufficient strength to remain attached to filopodia membranes in the presence of applied mechanical tension. Immediately following this membrane accumulation at the filopodial tips, the tips lifted off the substrate and elongated in RGCs treated with either 40 nm anti-Thy1 (Fig. 3a and

supplementary video 1, n>10) or 40 nm CtxB SPIONs (Figure 3b and supplementary video 2, n>10) but not after exposure to non-functionalized SPIONs (n>3; data not shown). When we used the 10 nm anti-Thy1 SPION, which generate smaller magnetic forces, filopodia elongation was also observed in all cases and was indistinguishable from the 40 nm cases (n>5; data not shown) demonstrating that filopodia elongation can be achieved with SPIONs that generate forces of 3–6 pNs. After elongation initiated, the rate of ongoing elongation could be regulated by reducing or increasing the voltage to the electromagnet, or by changing the distance between the electromagnet tip and the RGC filopodia-bound SPION. Since the electromagnet pole entered the dish at an angle, the magnetic field was not completely parallel to the dish surface and therefore, filopodia lifted off the substrate into a slightly different focal plane than the growth cone. It is essential to note that the electromagnet tip had to be well sharpened and placed ahead of the growth cone at approximately a 45 degree angle while physically contacting the bottom of the culture dish in order to induce filopodial elongation. This technique allows for sufficient SPION accumulation at the filopodial tip due to close proximity of the magnetic field to the growth cone. Notably, in all the experiments carried out for this study (n>30), not a single filopodium broke during the elongation process. Thus, in response to applied mechanical tension, filopodia reconfigure cellular membrane to elongate at high rates and avoid breakage.

Analyzing the 40nm CtxB SPION experiments in more detail, we observed that 30 ± 10% of the growth cone filopodia elongated. Filopodia closest to the electromagnet elongated more frequently, consistent with the stronger magnetic field and thus greater force applied at shorter distances from the electromagnet tip (Fig. 3c). The average distance from the electromagnet tip to the initial position of the tip of successfully elongated filopodia was 31±4.5 μm (Fig. 3c). The average speed of elongated filopodia during the CtxB SPION experiments was 10±5 μm/min.

Next, we studied the effect of filopodia elongation on the actin cytoskeleton. We asked whether elongating the filopodial membrane by magnetic tension allows actin filament polymerization in or transport into the elongated region of the filopodia. To label the RGC actin cytoskeleton, we overexpressed a fluorescent LifeAct peptide in RGCs, which binds to filamentous but not monomeric actin. To obtain optimal images of F-actin inside elongated filopodia, we anchored these filopodia to the magnet tip by coating the magnet tip with PDL and laminin and turned off the magnet, to avoid movement artifacts seen when the magnet is on. PDL-laminin effectively stabilized elongated filopodia and allowed us to detect the presence of F-actin filaments inside the elongated region of the filopodia (Fig. 4a, n=5).

The SPION/magnetic field system established here allowed us to test the hypothesis that filopodial tension promotes growth cone advance when filopodial integrins are linked to the substrate. First, to verify whether SPION-induced elongating filopodia are exerting retraction forces, we removed the magnetic force and analyzed the elongated filopodial response. We observed that just after removing the magnetic force, elongated filopodia were pulled back towards their original position (Fig. 3b, supplementary video 2, n>6). This result confirms that there is an accumulation of tension during the elongation process that induces filopodia to retract to their original position once the external force is removed. Thus, these

elongated filopodia are generating mechanical tension that could be transmitted to the growth cone to promote elongation.

To examine whether this filopodial tension is able to promote axon elongation when integrins are linked to the substrate, we anchored the tip of the elongated filopodia to the PDL-laminin electromagnet pole and focused on the response of the growth cone. After 30 minutes, growth cones remained at the same position (n>6, example in Fig. 4a) and only sporadically did we observe filopodia engorging and adapting their shape to the new anchorage point (as in Fig. 4b). Thus, filopodial retraction forces from elongated filopodia are unable to induce growth cone advance when filopodia integrin receptors are linked to a laminin substrate.

## Discussion

In this study, we have used SPION and magnetic fields to demonstrate that mechanical tension applied at the tip of neuronal growth cone filopodia is able to induce filopodia elongation, supporting the idea that an axial force against the tip of the filopodia is sufficient to effectively induce filopodia growth, consistent with the Brownian ratchet model.[18] In our experiments, the application of magnetic fields to SPIONs located at the RGC growth cone membrane produced accumulation of SPIONs at the filopodial tip, allowing us to apply mechanical tension specifically to this region. This observation parallels a recent report in which SPIONs directed to mast cell receptors caused them to cluster at the cell membrane when a focal magnetic field was applied,[37] and indicates that SPION linkage to the membrane using the surface functionalizations tested here is strong enough to maintain filopodial attachment in the presence of applied mechanical tension.

The pN forces produced at the filopodia tip result in the almost immediate elongation of the filopodia. The elongation rate achieved using this method is up to 20 times the rate of elongation in neuronal filopodia[38] and similar to the induced elongation rates obtained in macrophage filopodia using magnetic beads.[39] Thus, filopodia reorganize cellular membrane in response to applied mechanical tension, and elongate at high rates without breakage, consistent with data suggesting that tension-induced elongation is accompanied by active lipid transport to the plasma membrane.[40]

In our experiments, mechanical tension applied to the tip of the filopodia allows for the extension of the actin cytoskeleton inside the elongated portion of the filopodia. Actin polymerization in cells is limited by, among other factors, the physical barrier of the adjacent cellular membrane. Polymerization rate of actin monomers in vitro is reduced ten times when polymerization occurs inside a liposome membrane.[18, 19] According to the Brownian ratchet model,[18] the physical presence of the membrane at the end of the actin filament impairs the insertion of new actin monomers, reducing the resulting actin polymerization rate. In our experiments, relieving the cellular membrane tension at the filopodial tip may lead to an increase of actin polymerization by favoring the insertion of new actin monomers. Similarly, other data have shown that decreasing membrane tension by adding amphiphilic compounds increases lamellipodial extension rate.[41] Lastly, elongated filopodia are able to generate retrograde forces similar to the retraction forces observed by

other authors in naïve neuronal growth cone filopodia.[21, 30, 42, 43] Thus, our results confirm that elongated filopodia are active organelles capable of rapidly inducing polymerization, and generating retrograde forces, and are not simply elongated membrane tethers.

Data obtained in this study also counter the hypothesis that linking filopodial retrograde forces to the substrate through integrin receptors is sufficient to induce growth cone advance. Our experiments show that, although elongated filopodia were under mechanical tension, filled with actin filaments, and effectively anchored to the magnet tip with laminin (which binds integrin receptors), their corresponding growth cones did not advance towards the elongated filopodia location, even after 30 minutes. In contrast, chicken growth cone filopodia engorge and induce growth cone turning just few minutes after the filopodia contacts a signaling cue.[42] In some filopodia we observed filopodial engorgement, but these were still insufficient to induce effective growth cone advance. However, when the traction point of the mechanical tensions is expanded along the entire growth cone membrane either by attaching 5 μm diameter magnetic beads[24] or glass pipette tips,[21] or even by applying a vacuum,[44] the transmitted force is sufficient to induce axon growth. Similarly, mechanical tension applied at the axon shaft of cultured neurons by gradually opening a gap in the substrate between neuronal cell body and distal portion of the axon also induces axon growth.[25, 27] Thus, these results suggest that the structure of the filopodia by itself is not sufficient to transmit the force or signal sufficient to induce axon growth, and additional signaling pathways or structural components are required in filopodia to induce growth cone turning or advance. Interestingly, others have also suggested a more complex picture of the clutch model for growth cone advance in which other factors such as substrate stiffness,[30] filopodial adhesions[45] or signaling cascades that affect integrin coupling to actin filaments,[46] play a major role in growth cone advance.

Could SPIONs-induced axon manipulation have a role in vivo or translational potential? The failure of axon regeneration in the central nervous system, and incomplete regeneration in the peripheral nervous system, remain significant causes of morbidity. It is important to note that axon growth induced by applying mechanical tension has been achieved multiple times in vitro, but never in vivo. We envision a clinical application of SPIONs to induce axon growth in vivo. SPIONs are already used diagnostically in the clinic[47] and their small size permits diffusion or transport through tissues to reach CNS targets,[48] including at injured axons.[49] However, the data presented here indicate that it will be essential to apply mechanical tension at a specific location in the axon to induce axon growth. Next experiments should include assessing the ability of SPIONs to promote axon growth in vivo, to promote regeneration and circuit formation in the nervous system.

In summary, we have demonstrated SPIONs can be targeted specifically to molecules present in RGC membranes, and an external magnetic field can apply pN forces to these membrane-localized SPIONs to elicit filopodial elongation. These elongated filopodia extend their plasma membrane independent of chemical external cues and demonstrate rapid filling with cytoplasmic actin filaments, demonstrating that mechanical tension is sufficient to induce membrane and actin redistribution in growing filopodia. During elongation, filopodia continuously exert retraction forces that oppose elongation. However, elongation and stabilization of filopodia fail to induce growth cone advance, highlighting the

complexity of filopodia function and suggesting that additional structural components and/or signaling pathways are required in filopodia to promote growth cone advance.[31, 50] In conclusion, this study provides a tool for studying the role of mechanical forces in growth cone filopodia dynamics and function. Additionally, this technique could be adapted for studying other biological questions at the neuronal membrane like clustering of receptors at the filopodial tip. It will be important in future experiments to determine whether this approach can also be optimized to induce axon growth as a possible therapy for neurodegenerative diseases or injury where axon regeneration fails.

## Supplementary Material

Refer to Web version on PubMed Central for supplementary material.

## Acknowledgments

**Financial support:** Department of Defense USAMRAA (W81XWH-12-1-0254, JLG), NEI (EY017971, JLG and P30s EY022589 and EY014801), NIH NRSA T32NS007044 (MBS), the James and Esther King Foundation (Technology Transfer Feasibility Grant #2KF03), as well as an unrestricted grant from Research to Prevent Blindness, Inc. These funding sources did not play a role in designing and conducting the research, interpreting the data or writing the manuscript.

We gratefully acknowledge funding from the Department of Defense USAMRAA (W81XWH-12-1-0254, JLG) NEI (EY017971, JLG and P30s EY022589 and EY014801), NIH NRSA T32NS007044 (MBS), the James and Esther King Foundation (Technology Transfer Feasibility Grant #2KF03), as well as an unrestricted grant from Research to Prevent Blindness, Inc. We thank Amber Hackett for helpful comments on the manuscript and Margaret Bates for technical assistance with electron microscopy.

## Abbreviations

| | |
|---|---|
| **CNS** | Central Nervous system |
| **CtxB** | Cholera Toxin B |
| **PDL** | Poly-D-Lysine |
| **RGCs** | Retinal Ganglion Cells |
| **SPIONs** | Superparamagnetic iron oxide nanoparticles |
| **TEM** | Transmission electron microscopy |

## References

1. Goldberg JL, Klassen MP, Hua Y, Barres BA. Amacrine-signaled loss of intrinsic axon growth ability by retinal ganglion cells. Science. 2002; 296(5574):1860–4. [PubMed: 12052959]
2. Canty AJ, Huang L, Jackson JS, et al. In-vivo single neuron axotomy triggers axon regeneration to restore synaptic density in specific cortical circuits. Nat Commun. 2013; 4:2038. [PubMed: 23799397]
3. Goldberg JL, Espinosa JS, Xu Y, Davidson N, Kovacs GT, Barres BA. Retinal ganglion cells do not extend axons by default: promotion by neurotrophic signaling and electrical activity. Neuron. 2002; 33 (5):689–702. [PubMed: 11879647]
4. So KF, Aguayo AJ. Lengthy regrowth of cut axons from ganglion cells after peripheral nerve transplantation into the retina of adult rats. Brain Res. 1985; 328(2):349–54. [PubMed: 3986532]

5. Caroni P, Schwab ME. Antibody against myelin-associated inhibitor of neurite growth neutralizes nonpermissive substrate properties of CNS white matter. Neuron. 1988; 1(1):85–96. [PubMed: 3272156]
6. Savio T, Schwab ME. Lesioned corticospinal tract axons regenerate in myelin-free rat spinal cord. Proceedings of the National Academy of Sciences of the United States of America. 1990; 87(11): 4130–3. [PubMed: 2349222]
7. Fawcett JW, Asher RA. The glial scar and central nervous system repair. Brain Res Bull. 1999; 49 (6):377–91. [PubMed: 10483914]
8. Yin Y, Henzl MT, Lorber B, et al. Oncomodulin is a macrophage-derived signal for axon regeneration in retinal ganglion cells. Nature neuroscience. 2006; 9(6):843–52. [PubMed: 16699509]
9. Leibinger M, Muller A, Andreadaki A, Hauk TG, Kirsch M, Fischer D. Neuroprotective and axon growth-promoting effects following inflammatory stimulation on mature retinal ganglion cells in mice depend on ciliary neurotrophic factor and leukemia inhibitory factor. The Journal of neuroscience : the official journal of the Society for Neuroscience. 2009; 29(45):14334–41. [PubMed: 19906980]
10. Mansour-Robaey S, Clarke DB, Wang YC, Bray GM, Aguayo AJ. Effects of ocular injury and administration of brain-derived neurotrophic factor on survival and regrowth of axotomized retinal ganglion cells. Proceedings of the National Academy of Sciences of the United States of America. 1994; 91 (5):1632–6. [PubMed: 8127857]
11. Ellis-Behnke RG, Liang YX, You SW, et al. Nano neuro knitting: peptide nanofiber scaffold for brain repair and axon regeneration with functional return of vision. Proceedings of the National Academy of Sciences of the United States of America. 2006; 103(13):5054–9. [PubMed: 16549776]
12. Tysseling-Mattiace VM, Sahni V, Niece KL, et al. Self-assembling nanofibers inhibit glial scar formation and promote axon elongation after spinal cord injury. The Journal of neuroscience : the official journal of the Society for Neuroscience. 2008; 28(14):3814–23. [PubMed: 18385339]
13. Park KK, Liu K, Hu Y, et al. Promoting axon regeneration in the adult CNS by modulation of the PTEN/mTOR pathway. Science. 2008; 322(5903):963–6. [PubMed: 18988856]
14. Neumann S, Woolf CJ. Regeneration of dorsal column fibers into and beyond the lesion site following adult spinal cord injury. Neuron. 1999; 23(1):83–91. [PubMed: 10402195]
15. Sun F, Park KK, Belin S, et al. Sustained axon regeneration induced by co-deletion of PTEN and SOCS3. Nature. 2011; 480(7377):372–5. [PubMed: 22056987]
16. Luo X, Salgueiro Y, Beckerman SR, Lemmon VP, Tsoulfas P, Park KK. Three-dimensional evaluation of retinal ganglion cell axon regeneration and pathfinding in whole mouse tissue after injury. Experimental neurology. 2013; 247:653–62. [PubMed: 23510761]
17. Gallo G. Mechanisms underlying the initiation and dynamics of neuronal filopodia: from neurite formation to synaptogenesis. International review of cell and molecular biology. 2013; 301:95–156. [PubMed: 23317818]
18. Peskin CS, Odell GM, Oster GF. Cellular motions and thermal fluctuations: the Brownian ratchet. Biophysical journal. 1993; 65(1):316–24. [PubMed: 8369439]
19. Miyata H, Nishiyama S, Akashi K, Kinosita K Jr. Protrusive growth from giant liposomes driven by actin polymerization. Proceedings of the National Academy of Sciences of the United States of America. 1999; 96(5):2048–53. [PubMed: 10051592]
20. Bornschlogl T. How filopodia pull: what we know about the mechanics and dynamics of filopodia. Cytoskeleton. 2013; 70(10):590–603. [PubMed: 23959922]
21. Heidemann SR, Lamoureux P, Buxbaum RE. Growth cone behavior and production of traction force. The Journal of cell biology. 1990; 111(5 Pt 1):1949–57. [PubMed: 2229183]
22. Suter DM, Miller KE. The emerging role of forces in axonal elongation. Prog Neurobiol. 2011; 94 (2):91–101. [PubMed: 21527310]
23. Bray D. Axonal Growth in Response to Experimentally Applied Mechanical Tension. Developmental Biology. 1984; 102(2):379–89. [PubMed: 6706005]
24. Fass JN, Odde DJ. Tensile force-dependent neurite elicitation via anti-beta1 integrin antibody-coated magnetic beads. Biophysical journal. 2003; 85(1):623–36. [PubMed: 12829516]

25. Pfister BJ, Iwata A, Meaney DF, Smith DH. Extreme stretch growth of integrated axons. The Journal of neuroscience : the official journal of the Society for Neuroscience. 2004; 24(36):7978–83. [PubMed: 15356212]
26. Lamoureux P, Heidemann SR, Martzke NR, Miller KE. Growth and elongation within and along the axon. Dev Neurobiol. 2010; 70(3):135–49. [PubMed: 19950193]
27. Loverde JR, Tolentino RE, Pfister BJ. Axon stretch growth: the mechanotransduction of neuronal growth. Journal of visualized experiments : JoVE. 2011; (54)
28. Gomez TM, Letourneau PC. Actin dynamics in growth cone motility and navigation. Journal of neurochemistry. 2014; 129(2):221–34. [PubMed: 24164353]
29. Mitchison T, Kirschner M. Cytoskeletal dynamics and nerve growth. Neuron. 1988; 1(9):761–72. [PubMed: 3078414]
30. Chan CE, Odde DJ. Traction dynamics of filopodia on compliant substrates. Science. 2008; 322(5908):1687–91. [PubMed: 19074349]
31. Steketee MB, Moysidis SN, Jin XL, et al. Nanoparticle-mediated signaling endosome localization regulates growth cone motility and neurite growth. Proceedings of the National Academy of Sciences of the United States of America. 2011; 108(47):19042–7. [PubMed: 22065745]
32. Corredor RG, Trakhtenberg EF, Pita-Thomas W, Jin X, Hu Y, Goldberg JL. Soluble adenylyl cyclase activity is necessary for retinal ganglion cell survival and axon growth. The Journal of neuroscience : the official journal of the Society for Neuroscience. 2012; 32(22):7734–44. [PubMed: 22649251]
33. Trakhtenberg EF, Wang Y, Morkin MI, et al. Regulating Set-beta's Subcellular Localization Toggles Its Function between Inhibiting and Promoting Axon Growth and Regeneration. The Journal of neuroscience : the official journal of the Society for Neuroscience. 2014; 34(21):7361–74. [PubMed: 24849368]
34. Riedl J, Crevenna AH, Kessenbrock K, et al. Lifeact: a versatile marker to visualize F-actin. Nat Methods. 2008; 5(7):605–7. [PubMed: 18536722]
35. Hansson HA, Holmgren J, Svennerholm L. Ultrastructural localization of cell membrane GM1 ganglioside by cholera toxin. Proceedings of the National Academy of Sciences of the United States of America. 1977; 74(9):3782–6. [PubMed: 269432]
36. Beale R, Osborne NN. Localization of the Thy-1 antigen to the surfaces of rat retinal ganglion cells. Neurochem Int. 1982; 4(6):587–95. [PubMed: 20487915]
37. Mannix RJ, Kumar S, Cassiola F, et al. Nanomagnetic actuation of receptor-mediated signal transduction. Nat Nanotechnol. 2008; 3(1):36–40. [PubMed: 18654448]
38. Costantino S, Kent CB, Godin AG, Kennedy TE, Wiseman PW, Fournier AE. Semi-automated quantification of filopodial dynamics. Journal of neuroscience methods. 2008; 171(1):165–73. [PubMed: 18394712]
39. Zidovska A, Sackmann E. On the mechanical stabilization of filopodia. Biophysical journal. 2011; 100(6):1428–37. [PubMed: 21402024]
40. Forscher P, Lin CH, Thompson C. Novel form of growth cone motility involving site-directed actin filament assembly. Nature. 1992; 357(6378):515–8. [PubMed: 1608453]
41. Raucher D, Sheetz MP. Cell spreading and lamellipodial extension rate is regulated by membrane tension. The Journal of cell biology. 2000; 148(1):127–36. [PubMed: 10629223]
42. Gallo G, Lefcort FB, Letourneau PC. The trkA receptor mediates growth cone turning toward a localized source of nerve growth factor. The Journal of neuroscience : the official journal of the Society for Neuroscience. 1997; 17(14):5445–54. [PubMed: 9204927]
43. Steketee MB, Tosney KW. Contact with isolated sclerotome cells steers sensory growth cones by altering distinct elements of extension. The Journal of neuroscience : the official journal of the Society for Neuroscience. 1999; 19(9):3495–506. [PubMed: 10212309]
44. Nguyen TD, Hogue IB, Cung K, Purohit PK, McAlpine MC. Tension-induced neurite growth in microfluidic channels. Lab on a chip. 2013; 13(18):3735–40. [PubMed: 23884453]
45. Steketee MB, Tosney KW. Three functionally distinct adhesions in filopodia: shaft adhesions control lamellar extension. The Journal of neuroscience : the official journal of the Society for Neuroscience. 2002; 22(18):8071–83. [PubMed: 12223561]

46. Robles E, Gomez TM. Focal adhesion kinase signaling at sites of integrin-mediated adhesion controls axon pathfinding. Nature neuroscience. 2006; 9(10):1274–83. [PubMed: 16964253]

47. Stoll G, Bendszus M. New approaches to neuroimaging of central nervous system inflammation. Curr Opin Neurol. 2010; 23(3):282–6. [PubMed: 20168228]

48. Pita-Thomas DW, Goldberg JL. Nanotechnology and glaucoma: little particles for a big disease. Curr Opin Ophthalmol. 2013

49. Harrison J, Bartlett CA, Cowin G, et al. In vivo imaging and biodistribution of multimodal polymeric nanoparticles delivered to the optic nerve. Small. 2012; 8(10):1579–89. [PubMed: 22411702]

50. Steketee MB, Oboudiyat C, Daneman R, et al. Regulation of intrinsic axon growth ability at retinal ganglion cell growth cones. Investigative ophthalmology & visual science. 2014; 55(7):4369–77. [PubMed: 24906860]

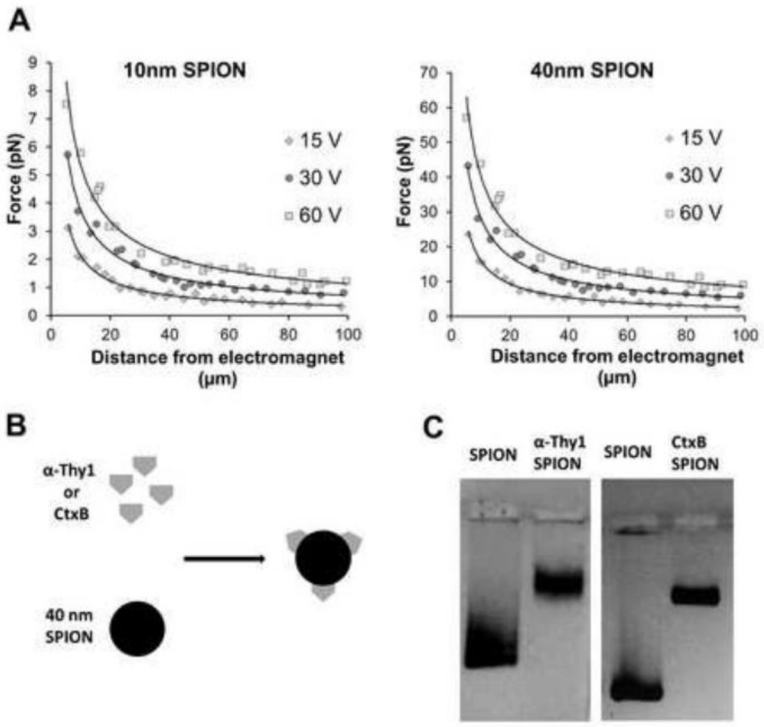


**Figure 1. SPION functionalization and properties**

(a) Forces generated by the electromagnet at different voltages and different distances from its tip with 10 nm and 40 nm diameter iron core SPIONs. (b) Diagram for 40 nm SPION chemical coupling to cholera toxin B or anti- (α-) Thy1 antibody. (c) Functionalized SPIONs migrate slower in agarose electrophoresis, demonstrating successful chemical coupling.

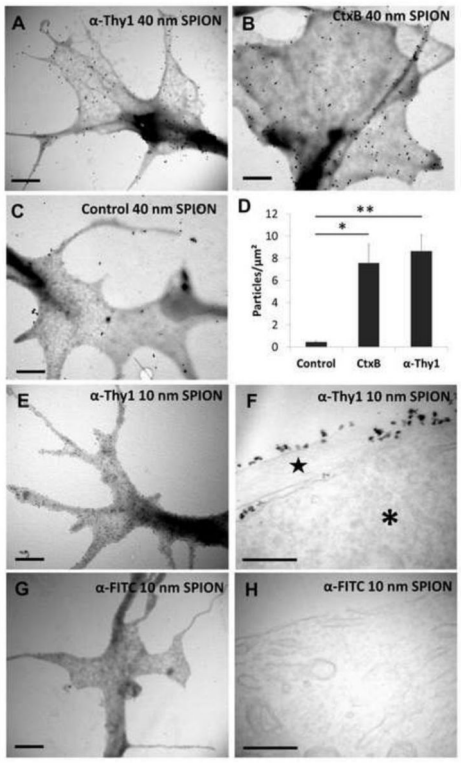


**Figure 2. Functionalized SPIONs attach to RGC membranes**

Transmitted electron microscope (TEM) images of RGC growth cones treated with (a) 40 nm anti-Thy1 SPIONs and (b) 40 nm anti-CtxB SPIONs for 30 minutes show abundant attachment of functionalized SPIONs to filopodia and other parts of the growth cone. (c) In contrast, very few non-functionalized 40 nm SPIONs are found at growth cone structures. (d) Quantification of number per surface unit of 40 nm iron core SPIONs functionalized with different moieties. Results are expressed as mean ± SEM of at least 4 growth cones in two independent experiments. Significance differences between functionalized and control non-functionalized SPIONs were tested using an unpaired Student's t-test. *$p<0.05$, **$p<0.01$. (e) TEM images of RGC growth cones incubated with 10 nm iron core anti-Thy1 SPIONs for 30 minutes show abundant SPION attachment. (f) TEM images of RGC microtome sections reveal that 10 nm iron core anti-Thy1 SPIONs remain on the outside membrane of the cell body (*) and neurite (star). (g) In contrast, 10 nm iron core anti-FITC SPIONs were not found in RGC growth cones nor in (h) RGC microtome sections. Scale bar 1 μm in a, b, c, e and g and 200 nm in f and h.

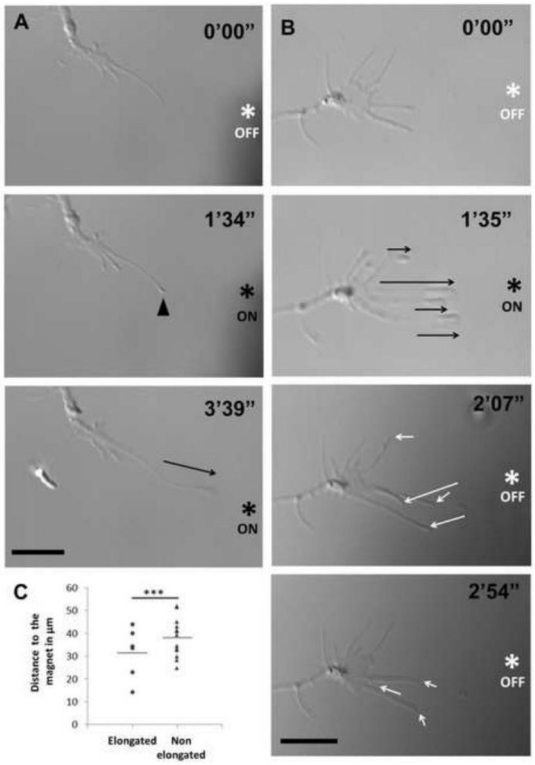


**Figure 3. Filopodia elongation and retraction in response to On/Off magnetic field**

(a) Filopodium from a cultured RGC treated with anti-thy1 SPION elongated (black arrow) towards the tip of the applied electromagnet (asterisk) during the first several minutes. An accumulation of membrane material in response to the magnetic field was observed at the tip of the filopodium (arrowhead) preceding elongation. (b) Similarly, in RGCs treated with CtxB SPIONs, several filopodia elongated (black arrows) in response to an applied magnetic field (ON). These filopodia rapidly retracted (white arrows) when the magnet was turned off (OFF). Scale bar 10 μm in a and b. (c) Distances from the end of each filopodium to the tip of the electromagnet were measured before elongation. From the total filopodia of a growth cone, the closest ones to the electromagnet tip were more likely to elongate towards the magnet (***$p<0.001$ by unpaired Student's t-test; n=6, 13; distances from tip of each filopodium to the magnet were normalized to the average distance of filopodia that elongated in that growth cone).

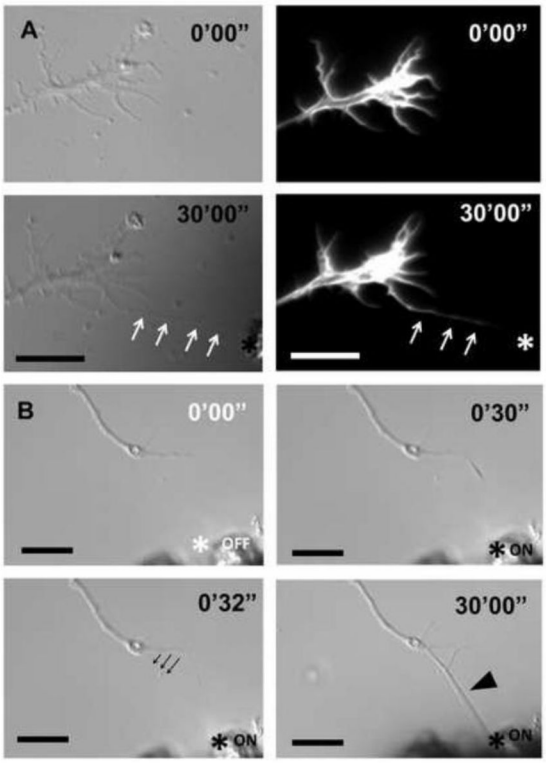


**Figure 4. Filopodial actin and growth cone responses to elongation**

(a) Thirty minutes after elongating a Thy1-SPION-treated filopodium to a PDL- and laminin-coated electromagnet tip (asterisk), the RGC growth cone did not change its position. Expression of RFP-LifeAct peptide in RGCs allowed visualization of F-actin filaments inside the elongated filopodium (white arrows). (b) A filopodium was elongated using CtxB-SPION, and anchored to the PDL-/laminin-coated electromagnet tip (asterisk). Engorgement of the filopodium after 30 minutes was observed (black arrowhead). The originating segment of the filopodium relocated to a new position (black arrows) in response to mechanical tension. Scale bar 10 μm in a and b.